At the onset of the island and especially at the point where the island reaches its marginal size the condition of a small island is by definition fulfilled. Taking $W_0 = 5.1(\chi_\perp/\chi_\parallel)^{1/4}(r_{res}L_q q/\varepsilon m)^{1/2}$, assuming a gyro-Bohm scaling ($\chi_\perp \sim T^{3/2}/B^2$) and taking the Spitzer formula $\chi_{Spitzer}$ for the parallel transport, Eq. (2b) is obtained. Within the island, the parallel transport $\chi_\parallel$ is reduced due to the heat flux limit [6] leading to $\beta^{\chi}_{p,marg} \sim \rho^*_{pi}$ [7].

It is important for the calculation of the bootstrap current to include the different influence from the density gradient ∇n and the temperature gradient ∇T in the calculation of L_p [8,3]. The corrected pressure gradient length according to [1] results in $1/L_p^{corr} \approx 1/3 \cdot 1/L_T + 2/3 \cdot 1/L_n$, which has been used within this work. The $T \cdot \nabla n$ term contributes stronger to the bootstrap current than the $n \cdot \nabla T$ term.

In order to fit $\beta_{p,onset}$ for the onset or the marginal $\beta_{p,marg}$, a simple power-law ansatz has been used. This ansatz is strictly only appropriate for fitting the data according to the $\chi_\perp/\chi_\parallel$-model as well as for the model by Poli [9] which both predict a power-law scaling.

Common discharge scenarios to determine the marginal β_p scaling For all three machines, AUG, DIII-D and JET, H-mode discharges with a JET-like low triangularity shape have been used. The main difference compared to the usual ASDEX Upgrade shape is at AUG a positive upper triangularity $\delta_{top} \approx 0.24$ which is typically around 0 at ASDEX Upgrade. The lower triangularity $\delta_{bottom} = 0.38$ is only slightly higher as in the usual ASDEX Upgrade case. The ellipticity $\kappa \approx 1.7$ is similar for both shapes. For ASDEX Upgrade and DIII-D purely NBI heating has been used, whereas for JET only at low $I_p \approx 1$ MA and $B_t \approx 1$ T NBI provided enough heating power to trigger a NTM reliably. At higher I_p, B_t values additional ICRH heating was applied in the early discharge phase to trigger the NTM with an early large sawtooth. After the onset of a (2/1)-NTM, which eventually locks, either by a $n = 1$ and/or locked mode detector for JET and DIII-D a preprogrammed NBI waveform for the power ramp has been triggered. At ASDEX Upgrade an entirely programmed waveform has been used (see fig. 1).

With increasing heating power, decreasing q_{95} or decreasing feedback controlled density and hence collisionality $\bar{\nu}_{ii}$ the (2/1)-NTM gets excited. The otherwise appearing (3/2)-NTM entered the database for the (3/2)-NTM β_p^{marg}-scaling [5]. Still at high heating power the (2/1)-NTM locks to the vessel and stops the entire toroidal plasma rotation. With the reduction of the NBI heating power the mode gets smaller and starts rotating again. At JET the locked mode caused a problem due to the strong loss of particle confinement leading to heating power trips avoiding the unlocking and reaching β_p^{marg}.

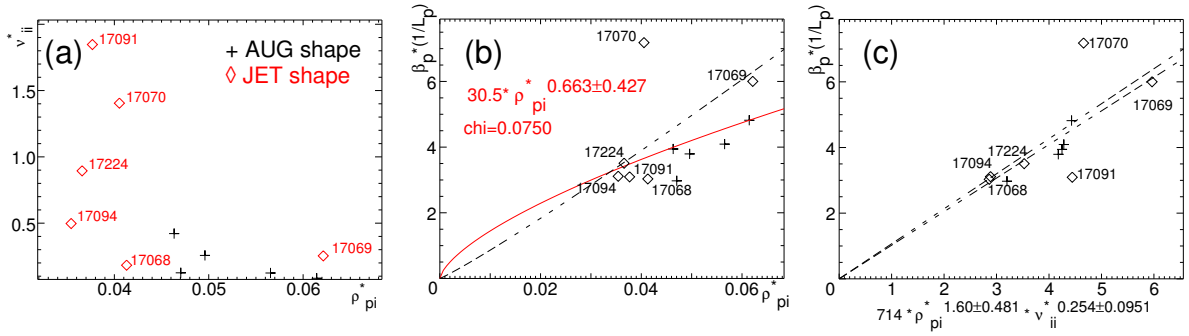

Figure 2: *Combined β_p^{marg}-scaling for ASDEX Upgrade (black crosses) and JET-like (red diamonds) ASDEX Upgrade type of discharges. Fig. (a) shows the parameter space in ρ^*_{pi} and $\bar{\nu}_{ii}$, fig. (b) the dependence of $\beta_p^{marg}/L_p^{corr}$ as function of ρ^*_{pi} and fig. (c) the full scaling with respect to ρ^*_{pi} and $\bar{\nu}_{ii}$.*

Importance of the calculation of L_p The uncorrected L_p can be used for the onset, as long as only discharges with negligible n_e-peaking at the time of the onset are considered. During the rampdown the ratio between the different terms significantly differs and L_p^{corr} gives the best results for the fitting of the temporal evolution of the mode amplitude as shown in fig. 3a and 3b [3]. For pellet triggered NTMs, either (3/2) or (2/1), a strong peaking of the density due to the pellets happens. This makes the use of L_p^{corr} also necessary for the NTM onset.

Scaling of the marginal β_p for the (2/1)-NTM The first data set for a β_p^{marg}-scaling for the (2/1)-

NTM at ASDEX Upgrade gave the scaling $\beta_p^{marg}/L_p^{corr}/\rho_{pi}^{*\,1.10\pm0.52} = 121\cdot\bar{\nu}_{ii}^{0.106\pm0.076}$ [3,4]. Adding the new JET-shaped data gave a clear extension of the parameter space (see fig. 2a), due to the fact, that the higher triangularity $\delta\approx 0.4$ compared to $\delta\approx 0.3$ results in a higher particle confinement time τ_p resulting in higher achievable densities and collisionalities $\bar{\nu}_{ii}$ and lower ρ_{pi}^*. With this combined data set, also spanning a wider range in $q_{95} = 3.8...5.5$, the following scaling (see fig. 2c) is obtained

$$\beta_p^{marg}/L_p^{corr}[2/1,AUG] = 714\cdot\rho_{pi}^{*\,1.60\pm0.48}\cdot\bar{\nu}_{ii}^{0.254\pm0.095}. \tag{3}$$

It must be noted that the ρ_{pi}^* dependence alone on the other hand gives a much smaller exponent, than the exponent found for the (3/2)-NTM (see fig. 2b).

Both for JET and DIII-D β_p^{marg} is typically reached just at the H to L backtransition. As this transition happens on a faster timescale than the typical decay time of the NTM, it is very difficult to fix the exact value of β_p^{marg} and the marginal island size W_{marg}. Additionally the profiles change rapidly. For ASDEX Upgrade the same situation occurs for low $q_{95} < 3.6$. For higher q_{95} the marginal β_p is reached well in H-mode.

Before combining the data from ASDEX Upgrade (AUG and JET shaping) and JET, the normalisation of ρ_{pi}^* has to be considered. The definitions $\rho_{pi}^*(AUG) = \rho_{pi}/a$ and $\rho_{pi}^*(JET) = \rho_{pi}/r_{res}$ differ typically by a factor of 2, due to the mode location and different machine sizes. For consistency the ASDEX Upgrade definition has been applied to the JET data. The definition $\rho_{pi}^*(AUG)$ does not contain information about the q-profile, whereas $\rho_{pi}^*(JET)$ contains the q-profile through r_{res}. For the JET (2/1) NTM data one finally arrives at

$$\beta_p^{marg}/L_p^{corr}[JET] = 39163\cdot\rho_{pi}^{*\,3.04\pm0.021}\cdot\bar{\nu}_{ii}^{0.0678\pm0.0057}.$$

The combined scaling law for the ASDEX Upgrade data and the JET data gives

$$\beta_p^{marg}/L_p^{corr}[AUG+JET] = 27359\cdot\rho_{pi}^{*\,2.76\pm0.27}\cdot\bar{\nu}_{ii}^{0.358\pm0.081}.$$

Both scalings are at present in contrast to previous results and should be treated with great care and considered as preliminary, as the number of data point is still very small and the scatter in the data pretty large. Also the DIII-D data has not yet been included in the combined scaling.

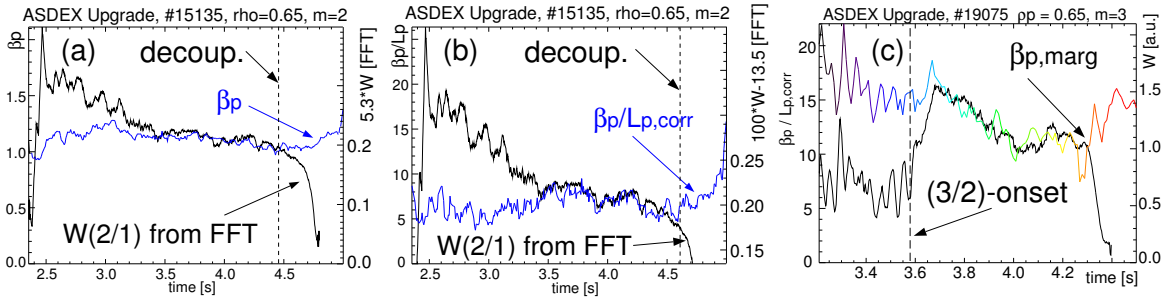

Figure 3: *Fig. (a) and (b) show the importance of using L_p^{corr} instead of just β_p or β_p/L_p for a (2/1)-NTM just after unlocking [4]. Fig. (c) shows the extreme case of a pellet triggered (3/2)-NTM, where after the last pellet triggering the NTM the profiles show a strong variation with respect to L_p^{corr}.*

Several arguments can be found for the unclear (2/1)-NTM scaling: The coupling of the (2/1) mode to the wall might add additional physics and an additional term in the Rutherford equation. With the large values of $\bar{\nu}_{ii}$ reached at the $q = 2$ surface it is unclear, if one is reaching the threshold-like behaviour of the g-function in $\bar{\nu}_{ii}$ [10,11]. This could no longer be described with a power-law assumption. Modes with different mode numbers are not required to have the same exponents in a power-law ansatz.

Extension of the parameter range in ρ_{pi}^* and $\bar{\nu}_{ii}$ for the NTM onset with pellets As presented in [12,6], pellets injected from the high field side may trigger NTMs. This typically happens in a two step proccess. The first pellets of a pellet sequence not only increase the density, but also lead to a strong peaking of the density [13]. The increased n_e rises the collisionality $\bar{\nu}_{ii}$ (fig. 4a). The peaking increases

the equilibrium bootstrap current significantly, as this depends strongly on the radial density gradient ∇n_e. The resulting reduction in the temperature lowers ρ^*_{pi} (fig. 4a) and hence β_p^{marg}. A subsequent pellet provides then the triggering seed-island.

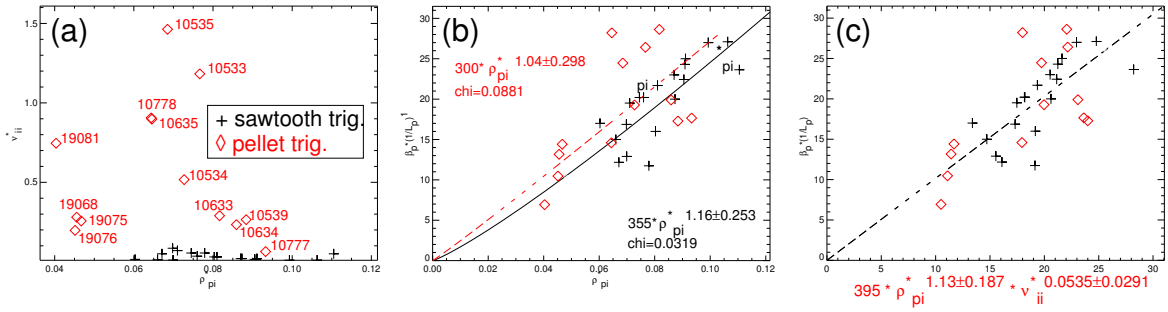

Figure 4: *Scaling of β_p^{onset} of pellet (red diamonds) and sawtooth (black crosses) triggered (3/2)-NTM. Fig. (a) shows the extended local parameter range in ρ^*_{pi} and $\bar{\nu}_{ii}$, fig. (b) shows the dependence of $\beta_p^{onset}/L_p^{corr}$ on ρ^*_{pi} alone and fig. (c) shows the full scaling with respect to ρ^*_{pi} and $\bar{\nu}_{ii}$.*

On-axis ICRH has been used to reduce the n_e-peaking in general [8] and has been used also in pellet fuelled discharges to avoid NTMs. In discharges reaching the highest β-values with pellets and unpeaked n_e-profiles NTMs can still be triggered. Combining conventionally and pellet triggered NTMs with and without ICRH the following onset scaling for the (3/2)-NTM is obtained (see fig. 4c)

$$\beta_p^{onset}/L_p^{corr}[3/2, AUG] = 395 \cdot {\rho^*_{pi}}^{1.13\pm0.19} \cdot \bar{\nu}_{ii}^{0.0535\pm0.0291}. \quad (4)$$

This scaling is consistent with previous results mainly influenced by ρ^*_{pi}. The pellet database alone results in a stronger collisionality dependence: $\beta_p^{onset}/L_p^{corr}[3/2, pellets] = 431 \cdot {\rho^*_{pi}}^{1.12\pm0.28} \cdot \bar{\nu}_{ii}^{0.156\pm0.091}$. The role and the mechanism for a NTM triggered by pellets needs to be discussed in more detail.

Summary and conclusions An attempt to extend the β_p^{marg}-scalings for the (2/1)-NTM by combining ASDEX Upgrade, DIII-D and JET data has been made. Using ASDEX Upgrade data with AUG and JET shapes extends the accessible paramater range and results in a larger collisionality impact and a higher ρ^*_{pi} exponent for the (2/1)-NTM. Including JET data gave no conclusive results yet and including DIII-D data had to be left as a future task. The high collisionalities $\bar{\nu}_{ii}$ question the validity of a power-law ansatz as one might reach the threshold behaviour. Including pellet triggered (3/2)-NTMs in the local scaling confirmed the linear ρ^*_{pi} dependence and a stronger $\bar{\nu}_{ii}$ influence. In all cases L_p^{corr} instead of L_p alone had to be used to fit the time evolution of the islands.

Acknowledgement O. Sauter has been supported by the Swiss National Science Foundation. The support and cooperation from all three machines is greatly appreciated.

References

[1] SAUTER, O. et al., Phys. Plasmas **6** (1999) 2834 .
[2] SAUTER, O. et al., Plasma Phys. Controlled Fusion **44** (2002) 1999 .
[3] MARASCHEK, M. et al., Plasma Phys. Controlled Fusion **45** (2003) 1369 .
[4] MARASCHEK, M. et al., in *30th EPS Conference, St. Petersburg*, volume 27A, page P1.120, 2003.
[5] BUTTERY, R. J. et al., 3/2 NTM metastability scaling towards ITER, in *this confernce*.
[6] ZOHM, H. et al., in *18th IAEA Conf., Sorrento, 2000*, pages IAEA–CN–77/EX3/1, 2000.
[7] ZOHM, H. et al., Phys. Plasmas **8** (2001) 2009.
[8] STOBER, J. et al., Plasma Phys. Controlled Fusion **43** (2001) A39.
[9] POLI, E. et al., Phys. Rev. Lett. **88** (2002) 075001.
[10] ZOHM, H. et al., Plasma Phys. Controlled Fusion **39** (1997) B237 .
[11] MARASCHEK, M. et al., Plasma Phys. Controlled Fusion **41** (1999) L1 .
[12] MARASCHEK, M. et al., in *Proc. 28th EPS, Madeira 2001*, volume 25A, pages 1801–1804.
[13] LANG, P. T. et al., Nucl. Fusion **40** (2000) 245.